ORIGINAL RESEARCH

High Prevalence of Pericardial Involvement in College Student Athletes Recovering From COVID-19

Daniel Brito, MD,[a],* Scott Meester, MD,[b],* Naveena Yanamala, MS, PhD,[a],* Heenaben B. Patel, MBBS,[a]
Brenden J. Balcik, MD,[b] Grace Casaclang-Verzosa, MD,[a] Karthik Seetharam, MD,[a] Diego Riveros, MD,[b]
Robert James Beto II, MD,[a] Sudarshan Balla, MD,[a] Aaron J. Monseau, MD,[b] Partho P. Sengupta, MD, DM[a]

ABSTRACT

OBJECTIVES This study sought to explore the spectrum of cardiac abnormalities in student athletes who returned to university campus in July 2020 with uncomplicated coronavirus disease 2019 (COVID-19).

BACKGROUND There is limited information on cardiovascular involvement in young individuals with mild or asymptomatic COVID-19.

METHODS Screening echocardiograms were performed in 54 consecutive student athletes (mean age 19 years; 85% male) who had positive results of reverse transcription polymerase chain reaction nasal swab testing of the upper respiratory tract or immunoglobulin G antibodies against severe acute respiratory syndrome coronavirus type 2. Sequential cardiac magnetic resonance imaging was performed in 48 (89%) subjects.

RESULTS A total of 16 (30%) athletes were asymptomatic, whereas 36 (66%) and 2 (4%) athletes reported mild and moderate COVID-19 related symptoms, respectively. For the 48 athletes completing both imaging studies, abnormal findings were identified in 27 (56.3%) individuals. This included 19 (39.5%) athletes with pericardial late enhancements with associated pericardial effusion. Of the individuals with pericardial enhancements, 6 (12.5%) had reduced global longitudinal strain and/or an increased native T_1. One patient showed myocardial enhancement, and reduced left ventricular ejection fraction or reduced global longitudinal strain with or without increased native T_1 values was also identified in an additional 7 (14.6%) individuals. Native T_2 findings were normal in all subjects, and no specific imaging features of myocardial inflammation were identified. Hierarchical clustering of left ventricular regional strain identified 3 unique myopericardial phenotypes that showed significant association with the cardiac magnetic resonance findings (p = 0.03).

CONCLUSIONS More than 1 in 3 previously healthy college athletes recovering from COVID-19 infection showed imaging features of a resolving pericardial inflammation. Although subtle changes in myocardial structure and function were identified, no athlete showed specific imaging features to suggest an ongoing myocarditis. Further studies are needed to understand the clinical implications and long-term evolution of these abnormalities in uncomplicated COVID-19. (J Am Coll Cardiol Img 2021;14:541–55) © 2021 Published by Elsevier on behalf of the American College of Cardiology Foundation.

**ABBREVIATIONS
AND ACRONYMS**

B-SSFP = balanced steady-
state free precession

CMR = cardiac magnetic
resonance

COVID-19 = coronavirus
disease-2019

ECG = electrocardiogram

EF = ejection fraction

GLS = global longitudinal
strain

IgG = immunoglobulin G

LGE = late gadolinium
enhancement

LV = left ventricular

PCR = polymerase chain
reaction

RV = right ventricular

SARS-CoV-2 = severe acute
respiratory syndrome-
coronavirus-2

STIR = short tau-axis inversion
recovery

Myocardial injury with an elevated troponin level may occur in 7% to 17% of patients hospitalized with coronavirus disease-2019 (COVID-19) and is present in 22% to 31% of those admitted to the intensive care unit (1–3). Although the mechanisms of myocardial injury are diverse, the clinical differentiation of severe acute respiratory syndrome-coronavirus-2 (SARS-CoV-2)– related myocarditis from other forms of myocardial dysfunction caused by hypoxia, inflammatory storm, or a stress cardiomyopathy- like presentation remains challenging. More recently, imaging studies have found changes in left ventricular (LV) and right ventricular (RV) structure and function in COVID-19 that can persist beyond the acute stage into several weeks and months of recovery (4). The immediate and long-term effects of these findings are unknown and warrant immediate scientific scrutiny.

With the infection's rapid spread throughout the community and the recent upsurge in COVID-19 in younger individuals, there is a potential need to understand the prevalence of any undiagnosed COVID-19-related cardiovascular involvement. Specifically, there is limited information regarding cardiac involvement among student athletes with mild or asymptomatic COVID-19 infection (5). This may be relevant for young college students and athletes who may be at a higher risk for sports- and exercise-related arrhythmias and cardiac dysfunction in the presence of underlying COVID-19- related myocardial injury. Therefore, our study aimed to investigate and determine the range of cardiac abnormalities seen in young athletes who had a diagnosis of mild or asymptomatic COVID-19 infection after returning to their college campus in July 2020. Using comprehensive echocardiography and cardiac magnetic resonance (CMR) imaging, we further investigated whether the pattern of echocardiographic involvement, including strain, could be associated with the COVID-19-related cardiac involvement observed on CMR.

METHODS

This cross-sectional observational study analyzed the data collected from college student athletes who returned to the West Virginia University, Morgantown (West Virginia) campus for the fall 2020 semester and were found to have COVID-19. A total of 160 athletes were tested between June 12 and August 4, 2020 (**Figure 1**). Initially, screening for COVID-19 by serum immunoglobulin G (IgG) antibody and nasopharyngeal swab testing for SARS-CoV-2 by real-time polymerase chain reaction (PCR) was performed on all athletes. IgG antibody testing was performed using a high-throughput chemiluminescent microparticle immunoassay with an ARCHITECT i2000SR immunoassay analyzer (Abbott, Abbott Park, Illinois) (6). The Sports Medicine Team at West Virginia University installed a monitoring protocol for the athletes that used a smartphone-developed application for recognizing COVID-19-related symptoms as defined by the Centers for Disease Control and Prevention (7). This questionnaire included the following symptoms: fever or chills, cough, shortness of breath, new onset of anosmia, fatigue, muscle or body aches, headache, sore throat, nasal congestion, nausea, vomiting, and/or diarrhea. In addition, athletes who initially tested negative were retested on a weekly basis by nasopharyngeal swab for SARS-CoV-2 by real-time PCR. Troponin-I was added to the panel of screening tests on all COVID-19-positive athletes, and additional tests such as C-reactive protein, erythrocyte sedimentation rate, and B-type natriuretic protein were evaluated as needed during individualized clinical assessments.

Following an appropriate quarantine period, an electrocardiogram (ECG) and comprehensive echocardiography were recommended in all patients; 54 underwent the tests. In addition, all patients who had symptomatic COVID-19 (n = 38) (**Figure 1**), and any asymptomatic (n = 16) patient with an abnormal ECG or an abnormal echocardiogram (i.e., abnormal global longitudinal strain [GLS] <16% or LV ejection fraction [EF] <50% or diagnostic uncertainty with echocardiographic features of RV dilation and/or RV dysfunction) underwent CMR imaging. We received exemption status from the Institutional Review Board of the West Virginia School of Medicine and followed guidelines issued by the Health Insurance Portability and Accountability Act Regulations, with all information collected from the electronic medical records after the patient's visit. Our research was performed within the ethical guidelines by the Declaration of Helsinki of 1975 (8).

ECHOCARDIOGRAPHY. Two-dimensional and Doppler echocardiographic examinations were performed using GE Vivid E9 (GE Healthcare, Chicago, Illinois) or Philips Epiq 7 (Philips, Amsterdam, the Netherlands) imaging systems equipped with 2.5-MHz and non-imaging transducers. Standard views were acquired, and right and left cardiac chamber quantification was performed according to the American Society of

FIGURE 1 COVID-19 Student Athlete Study Outline

Flowchart showing the flow and disposition of participants at each stage of the study. CMR = cardiac magnetic resonance; COVID-19 = coronavirus disease-2019; ECG = electrocardiogram; Echo = echocardiogram; IgG = immunoglobulin G; NP = nasopharyngeal; PCR = polymerase chain reaction.
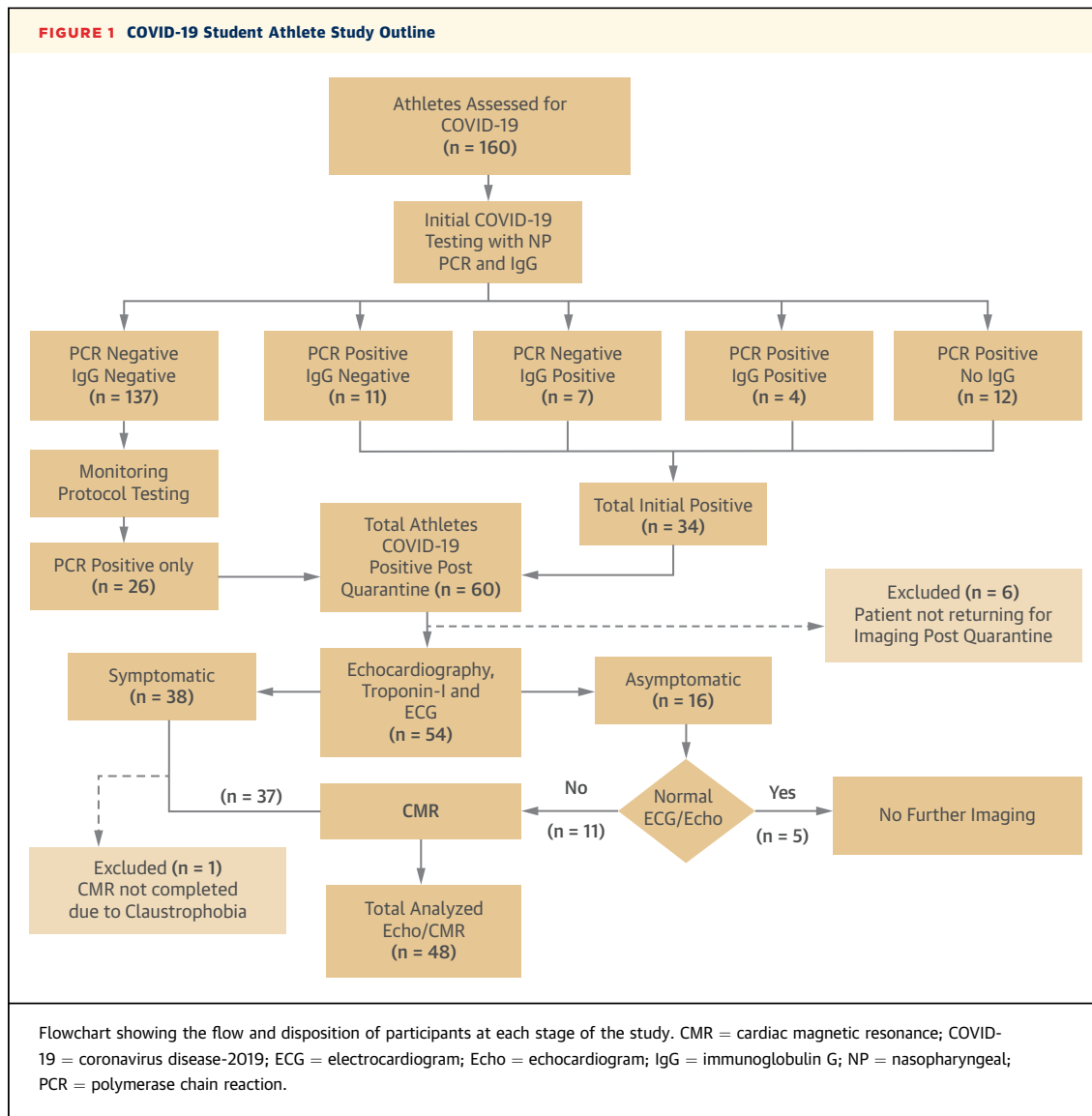
Echocardiography guidelines (9,10). The cutoff values for LV dysfunction (<50%) and RV dysfunction (RV fractional shortening <35%) were based on recommended guidelines (11,12).

SPECKLE TRACKING ECHOCARDIOGRAPHY. Speckle tracking analysis was performed in accordance with the American Society of Echocardiography recommendations by using off-line vendor-free software (ImageArena, TomTec, Inc., Hamden, Connecticut). Longitudinal strain was measured in all 3 views: apical 4-, 3-, and 2-chamber views. The peak GLS and regional longitudinal systolic strain were described using the 16-segment model. For LV GLS, an absolute magnitude lower than 16% was considered abnormal (12). The free wall of the right ventricle

was separated into 3 segments, which included the basal, middle, and apical regions. The strain value was calculated as the mean of the strain values present in the 3 segments, and an absolute value lower than 20% was considered abnormal (9,13).

CARDIAC MAGNETIC RESONANCE IMAGING. CMR was acquired on a 1.5-T magnet (Magnetom Aera, Siemens Medical Systems, Erlangen, Germany). Conventional sequences were obtained for imaging of cardiothoracic anatomy with axial stack of black blood using fast spin echo. Imaging for cardiac function, mass, and volume was performed using balanced steady-state free precession (B-SSFP) cine imaging. Tissue characterization of the left ventricle was performed with edema imaging, T_1 mapping, T_2 mapping, and

TABLE 1 Demographics and Clinical Characteristics in COVID-19–Negative and COVID-19–Positive (Symptomatic and Asymptomatic) Athletes

	COVID-19 Negative Control Athletes (n = 20)	COVID-19 Positive Athletes		p Value
		Symptomatic COVID-19 (n = 38 [70%])	Asymptomatic COVID-19 (n = 16 [30%])	
Age, yrs	20 (19–21)	19 (19–21)	19 (18–20)	0.41
Male	8 (40)	30 (79)	16 (100)	0.0001*
Race				0.007*
White	14 (70)	10 (26)	5 (31)	
African American	4 (20)	25 (66)	11 (69)	
Others	2 (10)	3 (8)	0 (0)	
BMI, kg/m^2	22.92 (21.33–25.70)	26.1† (24.7–29.5)	26.6† (24.8–28.3)	0.005‡
Sports				<0.0001*
Football	2 (10)	22 (58)	13 (81)	
Basketball	0 (0)	11 (29)	2 (13)	
Volleyball	0 (0)	1 (3)	0 (0)	
Soccer	5 (25)	2 (5)	0 (0)	
Swimming	0 (0)	0 (0)	1 (6)	
Others	13 (65)	2 (5)	0 (0)	
Cardiac symptoms	–	9 (24)	1 (6)	0.13
Vital signs				
Blood pressure, mm Hg				
SBP, mm Hg	119 (114–126)	130†§ (121–146)	136† (128–149)	0.0006‡
DBP, mm Hg	69 (64–80)	69.0 (63–80)	76 (67–81)	0.41
Heart rate, beats/min	62 (53–70)	65 (59–71)	60 (53–67)	0.31
ECG abnormalities	–	1 (3)	0 (0)	–
Laboratory testing				
Troponin-I >30, ng/l (n = 54)	–	1 (3)	0 (0)	–

Values are median (interquartile range) or n (%). *p < 0.05 using chi-square test. †p < 0.05 compared with the control group. ‡p < 0.05 using Kruskal-Wallis test with Dunn-Bonferroni correction. §p < 0.05 compared with the asymptomatic group.

BMI = body mass index; COVID-19 = coronavirus disease-2019; DBP = diastolic blood pressure; ECG = electrocardiographic; SBP = systolic blood pressure.

late gadolinium enhancement (LGE) imaging. Edema imaging was performed using T_2-weighted dark blood short tau inversion recovery (STIR) sequence. The acquired T_1 mapping was performed using the Shortened Modified Look Lockers Inversion (ShMOLLI) recovery sequence pre-contrast on 3 short-axis slices at the base, middle, and apical left ventricle, the same location as STIR images. T_2 map was performed using B-SSFP imaging with 3 different T_2 preparation times at the same locations as STIR images and T_1 maps (14). Late gadolinium imaging was performed 8 to 12 min after administration of the contrast agent (0.1 mmol/kg of gadobutrol [Gadavist], Bayer Healthcare, Whippany, New Jersey) (15).

CMR IMAGE ANALYSIS. Image analysis for LV volumes and function was performed using Vitrea software (Vital Images Inc., Minnetonka, Minnesota). Analysis of the short-axis images of T_1 map, T_2 map, and T_2-weighted images was performed as detailed here. T_2-weighted images were visually assessed for hyperintense areas. Analysis was performed to diagnose edema when the myocardial T_2 signal intensity ratio was ≥2:1 compared with that of skeletal muscle. Motion-corrected native T_1 images were post-processed using Vitrea software. To assess diffuse disease, a region of interest was drawn in the septum at the midcavity or basal cavity (if midcavity images were technically inadequate) in a short-axis image of the left ventricle in all patients for myocardial T_1 assessments (16). A previously published native T_2 value of more than 52 ms was considered abnormal (17). The estimated normal reference range and cutoff values for normal native T_1 were determined by using an age-matched group of 16 healthy individuals (Supplemental Table 1). On the basis of these data, a T_1 value of ≥990 ms was considered abnormal. Previous studies have suggested that the native T_1 values in age-matched healthy control subjects are slightly higher than in athletes (18), and therefore any values higher than those obtained in age-matched healthy control subjects can be considered abnormal.

In addition to the foregoing, parametric maps and segmental native T_1 relaxation times for the 16

TABLE 2 Echocardiographic Imaging Findings in COVID-19–Negative and COVID-19–Positive (Symptomatic and Asymptomatic) Athletes

	COVID-19-Negative Control Athletes (n = 20)	COVID-19-Positive Athletes		p Value
		Symptomatic COVID-19 (n = 38 [70%])	Asymptomatic COVID-19 (n = 16 [30%])	
Left heart				
IVSd (cm)	0.8 (0.7–1.0)	0.8 (0.7–1.0)	0.9 (0.8–1.0)	0.29
PWTd (cm)	0.9 (0.8–1.1)	1 (0.9–1.1)	0.95 (0.8–1.1)	0.28
LVIDd index (cm/m^2)	2.62 (2.56–2.75)	2.34*† (2.08–2.46)	2.43† (2.37–2.54)	0.0003‡
LVEDV index (ml/m^2)	67.77 (52.62–77.00)	61.04 (56.71–71.18)	71.43 (63.54–77.93)	0.08
LVESV index (ml/m^2)	26.61 (21.12–30.03)	25.65 (21.64–30.30)	29.28 (24.36–33.40)	0.26
LAVi (ml/m^2)	30.20 (24.87–35.02)	26.63 (21.68–31.88)	28.75 (26.86–33.15)	0.32
LVMi (g/m^2)	80.13 (66.48–96.58)	75.34 (62.60–90.78)	85.65 (73.51–97.70)	0.32
LVEF%	60.0 (57.5–62.7)	60.0 (55.0–64.0)	58.0 (54.0–61.5)	0.51
LVEF <50%	0 (0)	1 (3)	0 (0)	0.61
SVi (ml/m^2)	39.98 (32.89–46.26)	36.56 (33.09–42.99)	43.62 (34.49–47.27)	0.21
E/A ratio	1.8 (1.6–2.3)	1.8 (1.5–2.1)	2.05 (1.8–2.5)	0.12
Septal e' velocity (cm/s)	14.80 (12.03–15.76)	12.00*† (10.78–14.18)	14.10 (12.95–14.90)	0.008‡
Lateral e' velocity (cm/s)	20.00 (15.53–22.68)	17.40 (15.03–20.28)	19.05 (17.20–23.45)	0.13
Average e' velocity (cm/s)	17.90 (13.44–19.36)	14.90* (13.55–16.75)	16.38 (15.25–18.98)	0.028‡
E/e' ratio	5.91 (4.73–7.39)	6.21 (5.60–7.46)	6.91 (5.87–7.10)	0.31
Average E/e' ratio	5.3 (4.3–6.1)	5.5 (5.0–6.4)	5.7 (5.1–6.1)	0.31
LVGLS	22.8 (20.7–23.6)	21.7 (19.4–24.1)	21.4 (18.7–24.2)	0.24
LVGLS <16	0 (0)	4 (11)	2 (13)	0.28
Right heart				
RV dimension index (cm/m^2)	2.02 (1.78–2.17)	1.82*† (1.55–1.94)	1.98 (1.81–2.08)	0.006‡
RVFAC, %	43.08 (35.98–47.23)	23.23† (19.41–26.89)	26.40† (22.93–28.79)	<0.0001‡
RVFAC <35 %	4 (20)	34 (89)	15 (94)	<0.0001§
S', cm/s	14.00 (13.00–16.00)	14 (12.75–15.05)	13.85 (12.95–15.00)	0.95
RVFWLS, %	26.85 (23.80–32.10)	26.80 (22.18–30.55)	28.05 (23.15–30.05)	0.91
RVFWLS <20%	1 (5)	3 (8)	1 (6)	0.91
Small pericardial effusion ≥5 mm	0 (0)	2 (5)	1 (6)	0.55

Values are median (interquartile range) or n (%). *p < 0.05 compared with the asymptomatic group. †p < 0.05 compared with the control group. ‡p < 0.05 using Kruskal-Wallis test with Dunn-Bonferroni correction. §p < 0.05 using chi-square test.

A = late diastolic atrial contraction mitral wave velocity; COVID-19 = coronavirus disease-2019; E = early diastolic mitral wave velocity; e' = tissue Doppler–derived early diastolic mitral annular velocity; IVSd = interventricular septal thickness at end-diastole; LAVi = left atrium volume index; LV GLS = left ventricular global longitudinal strain; LVEDV = left ventricular end-diastolic volume, LVEF = left ventricular ejection fraction; LVESV = left ventricular end-systolic volume; LVIDd = left ventricular internal diameter end-diastole, LVMi = LV mass index; PWTd = posterior left ventricular wall thickness at end-diastole; RVFAC = right ventricular fractional area change; RVFWLS = RV free wall strain; S' = systolic excursion velocity; SVi = stroke volume index.

myocardial segments were obtained by post-processing the 3 short-axis slices to assess regional disease (cvi42, Circle Cardiovascular Imaging, Calgary, Canada). Care was taken to avoid blood pool contamination when contouring the epicardial and endocardial borders. For T_2 mapping, the endocardium and epicardial contouring was performed for the basal and midventricular short-axis slices. The apical slice was disregarded, and segments with artifacts were also excluded. NativeT_2 relaxation time per segment was quantitated on the motion-corrected images by using cvi42 software (Circle Cardiovascular Imaging). Imaging for myocardial scar and pericardial involvement was performed using a LGE technique at the same location as cine images. Late enhancement was qualitatively assessed visually. Pericardial enhancement was considered if there was involvement of the pericardial layers and was confirmed by 2

observers. T_1 map and B-SSFP cine images were used to differentiate fat tissue carefully from pericardial enhancement (Videos 1 to 3).

INTEGRATED MULTIMODALITY ADJUDICATION OF ABNORMALITIES. CMR features specific to myocardial inflammation required the presence of at least 1 T_2 criterion (global or regional increase of myocardial T_2 relaxation time or an increased signal intensity in T_2-weighted CMR images) and 1 T_1 criterion (an increased myocardial T_1, or LGE) (19). In addition, the abnormalities seen on echocardiography and CMR were integrated and adjudicated as follows: 1) pericardial: defined as the presence of late enhancement with pericardial effusion on CMR; 2) myocardial: presence of any of the following criteria in isolation or in a combination: a) LVEF <50%, b) presence of regional wall motion abnormality, c) GLS <16%, and

TABLE 3   CMR Imaging Findings COVID-19–Positive Athletes

	Overall (N = 48)	Symptomatic COVID-19 (n = 37 [77])	Asymptomatic COVID-19 (n = 11 [23])	p Value
Left heart				
LVEF, %	59.91 (56.64–62.88)	60.32 (56.66–63.33)	59.09 (54.79–61.64)	0.32
LVEF <50 %	1 (2)	1 (3)	0 (0)	
LVEDV index, ml/m^2	105.29 (94.15–117.73)	104.74 (93.09–117.17)	114.44 (99.52–118.69)	0.11
LVESV index, ml/m^2	41.7 (37.49–47.72)	39.81 (37.17–45.38)	46.82 (41.18–50.44)	0.02*
Right heart				
RVEF%	53.58 (48.33–59.43)	54.60 (47.55–59.77)	51.32 (50.82–57.22)	0.74
RVEDV index, ml/m^2	95.21 (86.69–106.93)	92.40 (82.91–107.33)	99.82 (95.46–105.28)	0.08
RVESV index, ml/m^2	44.12 (37.57–50.68)	43.2 (36.76–51.27)	46.80 (43.44–48.16)	0.19
Native T$_1$, ms	969.0 (950.0–984.0)	973.0 (950.0–984.75)	963.0 (951.3–974.0)	0.54
Abnormal native T$_1$ ≥990 ms	9 (19)	8 (22)	1 (9)	0.66
Upper tercile native T$_1$	15 (31)	13 (35)	2 (18)	0.46
Native T$_2$, ms	44.00 (42.00–45.00)	44.00 (42.00–45.00)	44.00 (42.00–44.75)	0.53
Abnormal native T$_2$, >52 ms	0 (0)	0 (0)	0 (0)	
Upper tercile native T$_2$	6 (13)	6 (16)	0 (0)	0.31
LGE	1 (2)	1 (3)	0 (0)	
Pericardial enhancement	19 (40)	10 (27)	9 (82)	0.003*
Small pericardial effusion ≥5 mm	28 (58)	20 (54)	8 (73)	0.31

Values are median (interquartile range) or n (%). *p < 0.05 between the symptomatic and asymptomatic COVID-19 group. The p values were calculated using Mann-Whitney U test where median is reported and the Fisher exact test where frequencies are reported.

LGE = late gadolinium enhancement; RVEDV = right ventricular end-diastolic volume; RVEF = right ventricular ejection fraction; RVESV = right ventricular end-systolic volume; other abbreviations as in **Table 2**.

d) native T$_1$ increase ≥990 ms; and 3) myopericardial: a combination of items 1 and 2.

STATISTICAL ANALYSIS. As a first step, we performed the Shapiro-Wilk test to check whether the data were normally distributed across different groups. We found that most of the variables were not normally distributed; therefore, we used nonparametric methods for all statistical analyses. Continuous data were expressed as the median (interquartile range). Categorical data were presented as counts (percentages). Comparisons of continuous variables of demographics, echocardiography, and CMR among different groups (i.e., control subjects, symptomatic COVID-19-positive student athletes, and asymptomatic COVID-19-positive student athletes) were performed using either the Kruskal-Wallis test with Dunn-Bonferroni correction or the Mann-Whitney U test. A chi-square test was used for categorical variables with an expected value for each cell to be 5 or greater. If this assumption was not met, a Fisher exact test was used. To investigate the relationship between regional strain and CMR, hierarchical cluster analysis was performed to identify relationships among the 16 segmental longitudinal strains that could otherwise remain undiscovered (additional details are presented in Supplemental Methods section). All statistical analyses were performed using Medcalc for Windows version 19.5.2 (MedCalc Software, Ostend, Belgium) and RStudio version 3.1.3 (R Foundation, Vienna, Austria). Statistical significance <0.05 was used for all tests.

RESULTS

A total of 160 student athletes were screened for COVID-19;53 (33.1%) tested positive on PCR, whereas 7 (4.3%) athletes tested positive for IgG antibodies against SARS-CoV-2 (Figure 1). A total of 4 (2.5%) individuals had positive results on both PCR and IgG antibody tests. By August 9, 2020, a total of 54 college-level athletes with COVID-19 had undergone imaging studies (Table 1). The median time interval from tests performed to the imaging assessment was 27 days (range 22 to 33 days). Overall, the median age was 19 years (range: 19 to 21 years), and more than 85% of the cohort was male. A total 36 (66%) and 2 (4%) individuals experienced mild and moderate COVID-19-related symptoms, respectively; however, the illness was self-limited, and none of the participants required hospitalization (20). The remaining 16 (30%) athletes reported no symptoms at the time of COVID-19 screening.

Nearly one-fourth of the symptomatic COVID-19 patients also experienced cardiac symptoms (shortness of breath, fatigue, chest pain, or lightheadedness), whereas only 1 (6%) of the patients with no specific COVID-19 symptoms, as defined by the

FIGURE 2 Symptomatic COVID-19 Athlete With Cardiac Involvement
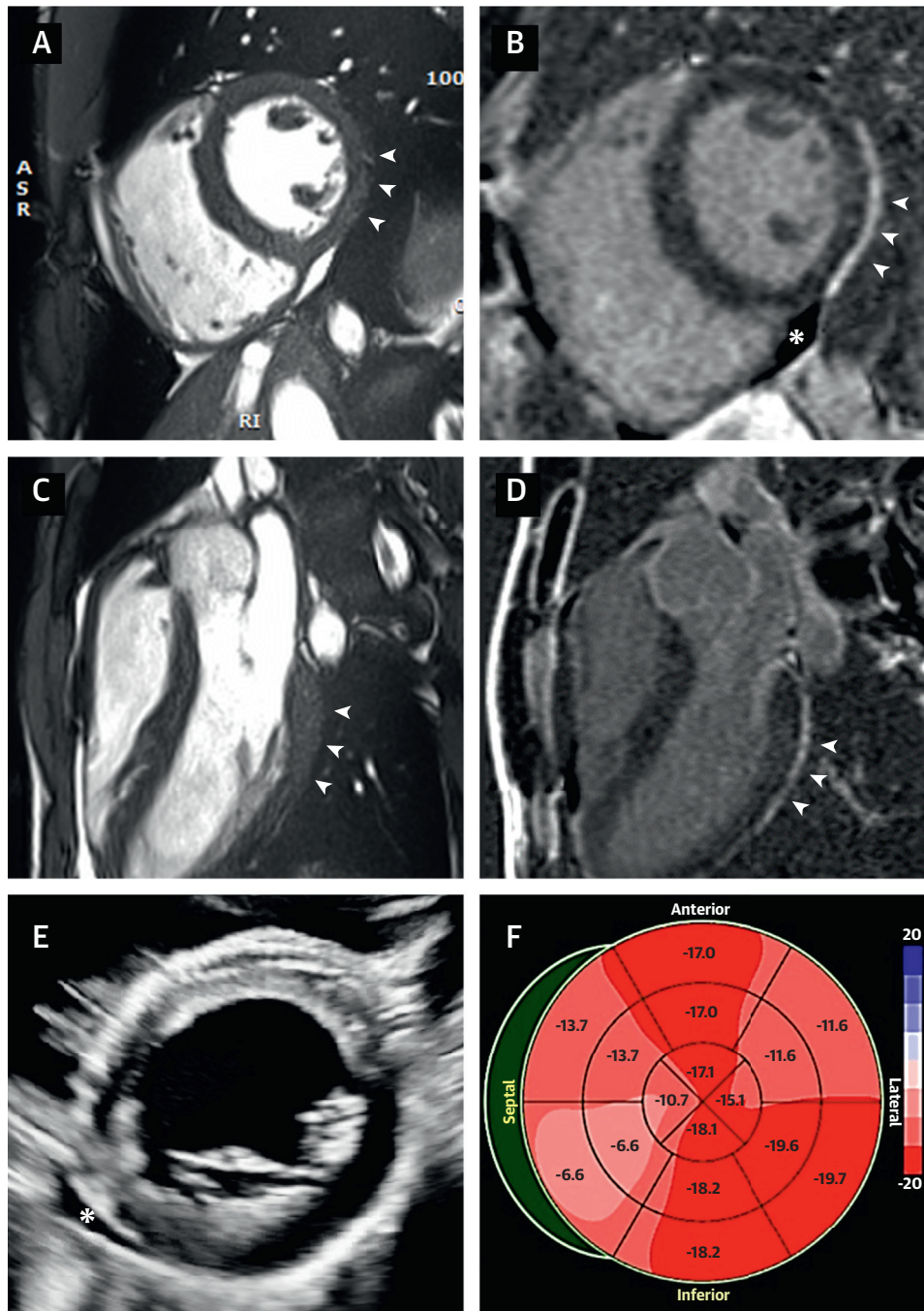
(A) Steady-state free precession cardiac magnetic resonance cine still frame in the midventricular short-axis view showing an absence of fat tissue **(arrowheads)** along the pericardial lining (Video 1). **(B)** Cardiac magnetic resonance phase-segmented inversion recovery sequence in the midventricular short-axis view demonstrates pericardial enhancement in the inferolateral wall **(arrowheads),** as well as a pericardial effusion (10.3 mm), localized inferiorly **(asterisk). (C and D)** Steady-state free precession and phase-segmented inversion recovery sequence in 3-chamber view again confirmed the presence of pericardial enhancement **(arrowheads in D)** and the lack of fat signal **(arrowheads in C)** (Video 2). **(E)** A 2-dimensional echocardiogram in the parasternal short-axis view was concordant with a small pericardial effusion localized inferiorly **(asterisk). (F)** A significant reduction in global longitudinal strain (14.5%) was recorded. Native T_1 relaxation time of the myocardium was increased at 997 ms. ASR = anterior right superior; COVID-19 = coronavirus disease-2019; RI = right inferior.

FIGURE 3   Two Asymptomatic COVID-19 Athletes With Cardiac Involvement
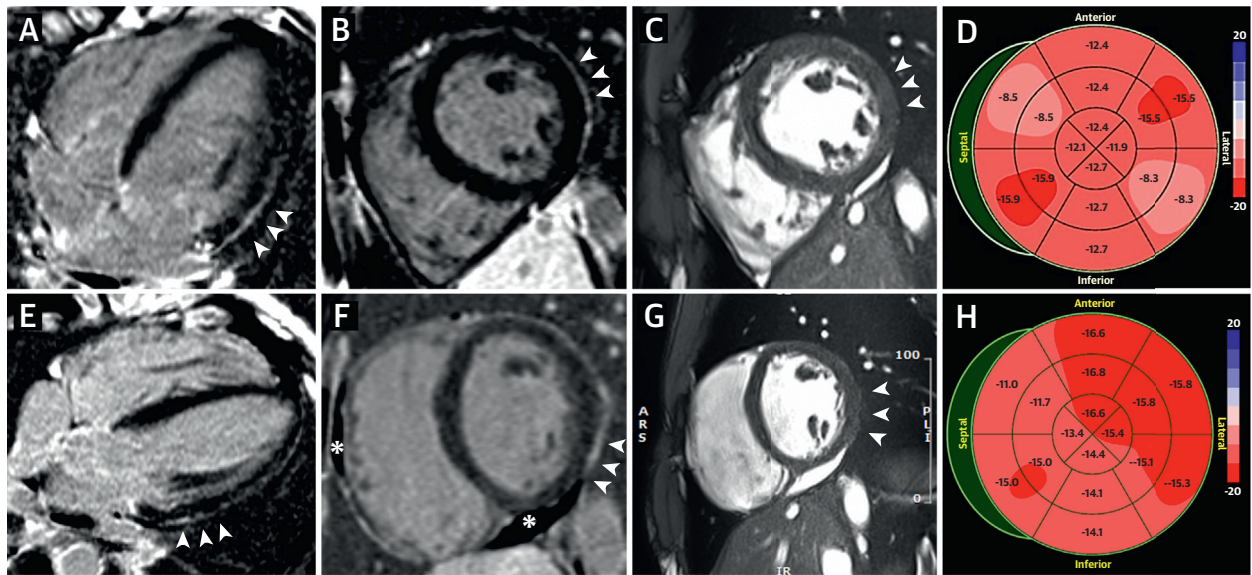
(A to D) Patient #1: cardiac magnetic resonance phase-segmented inversion recovery sequences demonstrated pericardial enhancement in the basal to middle anterolateral wall of the left ventricle **(arrowheads). (A)** 4-chamber view. **(B)** Short-axis view. **(C)** Steady-state free precession cardiac magnetic resonance cine still frame in the midventricular short-axis view demonstrating a lack of fat tissue signal (Video 3). **(D)** Despite a normal left ventricular ejection fraction (57%) and the absence of any myocardial involvement on cardiac magnetic resonance (native T_1 relaxation time assessed from left ventricular midseptal segments was normal at 950 ms), speckle tracking imaging–derived left ventricular global longitudinal strain was reduced (12.2%). **(E to H)** Patient #2: phase-segmented inversion recovery sequences on cardiac magnetic resonance demonstrating pericardial enhancement **(arrowheads)** in the anterolateral wall of the left ventricle and pockets of pericardial effusion (10.3 mm, **F**) localized inferiorly and anteriorly **(asterisk). (G)** Native. Despite a normal left ventricular ejection fraction (60%) and the absence of any myocardial involvement on cardiac magnetic resonance (native T_1 relaxation time assessed from left ventricular midseptal segments was normal at 963 ms), speckle tracking imaging–derived left ventricular global longitudinal strain was reduced (14.2%). ARS = anterior right superior; COVID-19 = coronavirus disease-2019; PLI = posterior left inferior.

Centers for Disease Control and Prevention guideline (7), subsequently reported a single episode of chest pain during the quarantine period. Cardiac troponin-I levels were normal except in 1 symptomatic patient (**Table 1**).

ABNORMAL ECHOCARDIOGRAPHIC FINDINGS. Cardiac wall and cavity dimensions, volume, LV mass index, and LVEF were similar in asymptomatic and symptomatic groups (**Table 2**). Symptomatic COVID-19 student athletes had significantly lower septal e′ (p = 0.008 vs. asymptomatic) and average e′ (p = 0.014 vs. asymptomatic) but not significantly lower lateral e′ velocities (p = 0.07). However, despite the significant group differences, these values are mostly within normal range for athletes and the general population. One symptomatic patient had an EF <50% with global hypokinesis (11). A total of 4 (11%) and 2 (13%) patients from the symptomatic and asymptomatic groups, respectively, had reduced GLS. There were no significant differences in the GLS or RV strain (**Table 2**). Small pericardial effusions (≥5 mm) were detected in 3 individuals. The importance

of the described echocardiographic findings in student athletes with COVID-19 is underlined by the comparison of age-matched athletic control subjects (n = 20) showing normal findings of LV structure and function in otherwise healthy noninfected athletes (**Table 2**).

ABNORMAL CMR FINDINGS. A total of 48 athletes underwent CMR. This group included all patients with symptomatic COVID-19 except 1, who could not complete CMR because of claustrophobia (n=37) (**Figure 1**). A total of 11 asymptomatic athletes underwent CMR, including the following: 1 with an abnormal ECG (inappropriate sinus tachycardia with ST-segment and T-wave changes); 2 with echocardiographically impaired LV function (abnormal GLS <16% or EF <50%); and 8 with borderline RV dilation or dysfunction on echocardiography (n = 8) necessitating CMR for overcoming diagnostic uncertainty.

Consistent with echocardiographic findings, no significant differences were noted between symptomatic and asymptomatic athletes with COVID-19

FIGURE 4 Pericardial Effusions in 2 Asymptomatic Athletes
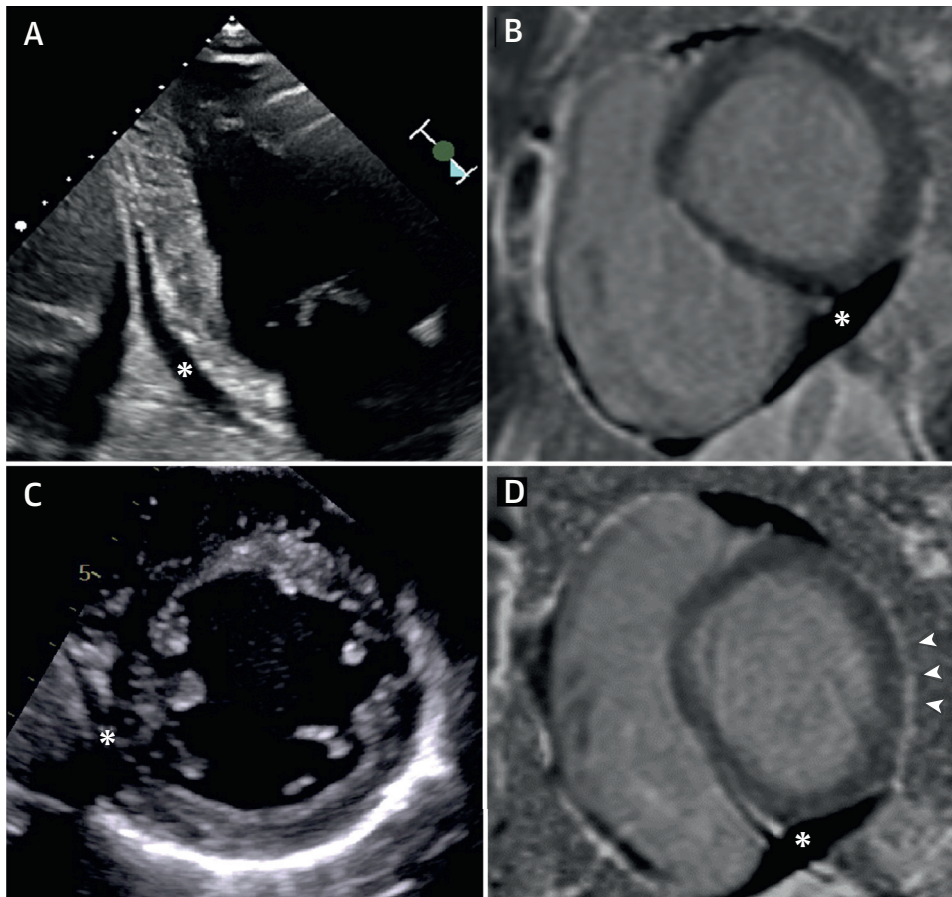
(A and B) Echocardiography in the apical 2-chamber view and the cardiac magnetic resonance phase-segmented inversion recovery sequence short-axis view showing pericardial effusion located inferiorly and anteriorly, respectively (2-dimensional echocardiography: 6.5 mm; cardiac magnetic resonance: 10.6 mm; **asterisk**). **(C and D)** A second athlete with pericardial effusion seen on echocardiography and cardiac magnetic resonance **(asterisk)**. The inferior pocket measured 12.7 mm. In addition, note the pericardial enhancement **(arrowheads)**.

(**Table 3**). One symptomatic patient had global LV hypokinesis with a reduced LVEF. Native T_2 values were normal in both groups, and CMR T_2-weighted STIR images showed an absence of myocardial edema in all cases. A total of 19 (40%) patients had late pericardial enhancement. Pericardial enhancement involved the lateral pericardium in a majority of patients. Pockets of pericardial effusion (≥5 mm) were identified in 28 (58%) patients (**Figures 2A to 4D**). Increased T_1 (≥990 ms) was seen in 9 (19%) athletes, with 1 symptomatic patient showing late myocardial enhancement (**Figures 5A to 5F**, Supplemental Figure 1).

INTEGRATED MULTIMODALITY ADJUDICATION.
The **Central Illustration** shows the overall prevalence of cardiac abnormalities as identified using echocardiography and CMR in 27 (56.3%) of 48 athletes. The frequency of abnormalities seen in the individual modalities are shown in Supplemental Table 2. In these 27 patients, the most common involvement was pericardial disease, with pericardial enhancement seen in 13 (48%). Specific CMR signs of myocardial inflammation (both T_1 and T_2 criteria) were not seen in any patient. A total of 6 (22.2%) patients with pericardial enhancement also showed additional myocardial abnormalities (GLS <16% [n = 2] or a native T_1 increase ≥990 ms [n = 3] or combination of both [n = 1]). Isolated myocardial involvement was seen in 8 (29.6%) patients (1 with LVEF <50%, 2 with GLS <16%, 4 with raised T_1, and 1 with GLS <16%, myocardial enhancement, and raised T1).

FIGURE 5 CMR End-Diastolic Frame From Cine, ShMOLLI Noncontrast T1 Map
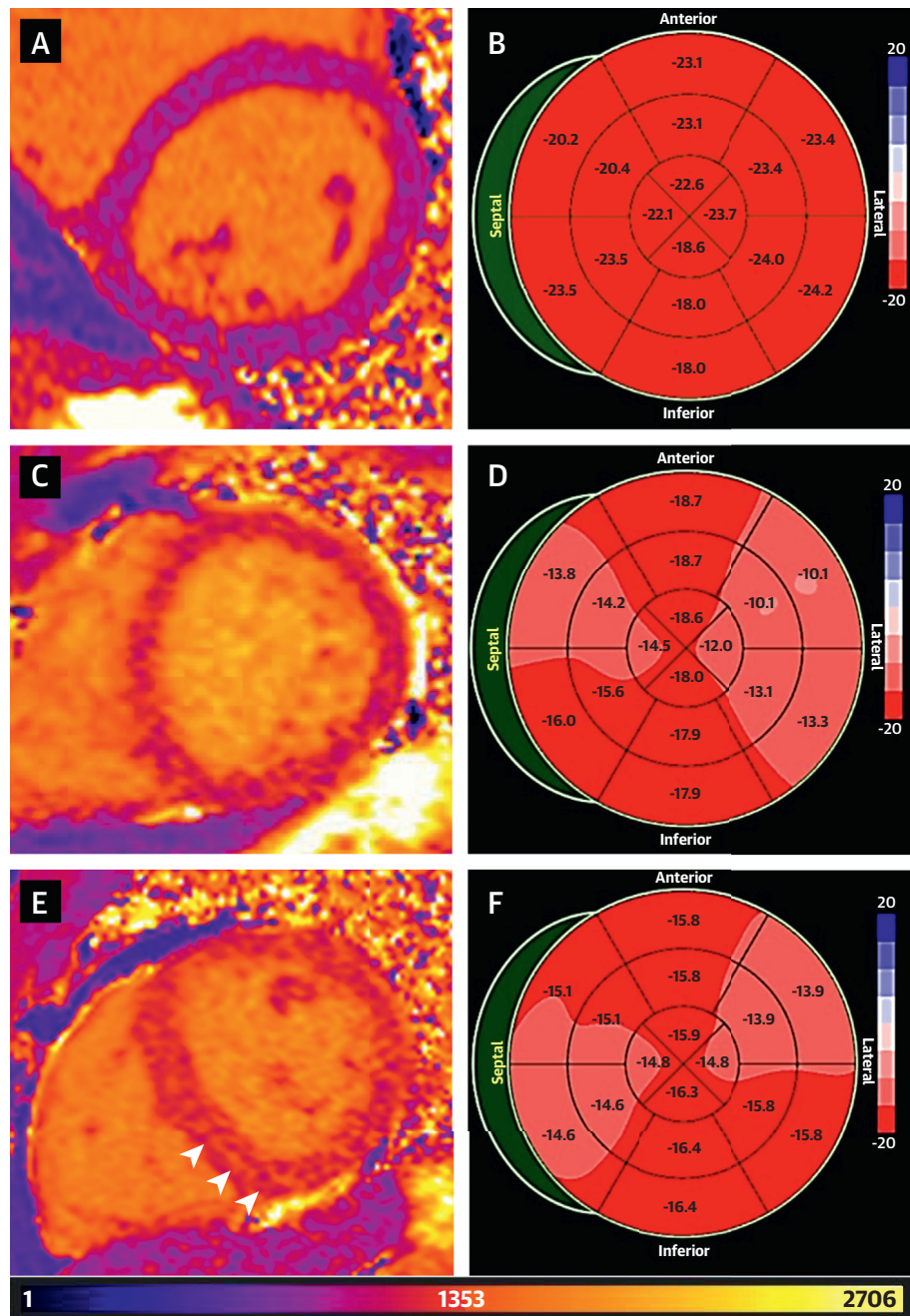
(A and B) Patient #1: A young asymptomatic athlete with evidence of normal findings on a cardiac magnetic resonance (CMR) native T_1 myocardial parametric map (midseptum, 927 ms) in (A) the mid-short-axis view, as well as (B) a normal 2-dimensional speckle tracking echocardiography–derived segmental strain pattern of the left ventricle (global longitudinal strain: 22.1%). (C and D) Patient #2: myocardial involvement in a symptomatic young athlete with a coronavirus disease 2019 diagnosis shows increased native T_1 (note the diffuse increase in T_1 appreciated as a red-orange color change in the T_1 map and measured in the midseptum as 1,001 ms). (D) The left ventricle also showed a significantly reduced global longitudinal strain (15%). (E and F) Patient #3: Myocardial involvement in a symptomatic young athlete. Cardiac magnetic resonance native T_1 map with evidence of midmyocardial enhancement (**arrowheads;** this is also appreciated in the 4-chamber view) (Supplemental Figure 1) in the inferoseptal wall of the left ventricle With diffuse increased native T_1 (measured in the midseptum as 992 ms) and (F) the left ventricle showing reduced global longitudinal strain (15.3%). ShMOLLI = Shortened Modified Look Lockers Inversion.

CENTRAL ILLUSTRATION Abnormal Findings of Pericardial, Myocardial, and Myopericardial Involvement in Mild Symptomatic and Asymptomatic Athletes With COVID-19

Abnormalities

Overall Group:
- Pericardial: 27.1%
- Myocardial: 16.7%
- Myopericardial: 12.5%

Symptomatic:
- Pericardial: 14.6%
- Myocardial: 16.7%
- Myopericardial: 6.25%

Asymptomatic:
- Pericardial: 12.5%
- Myopericardial: 6.25%

% of Total Patients (n = 48)

■ Late Gadolinium Enhancement Involving Pericardium
■ ↓EF/↑Native T1/↓Global Longitudinal Strain/ Late Gadolinium Enhancement Involving Myocardium
■ Combination of Both
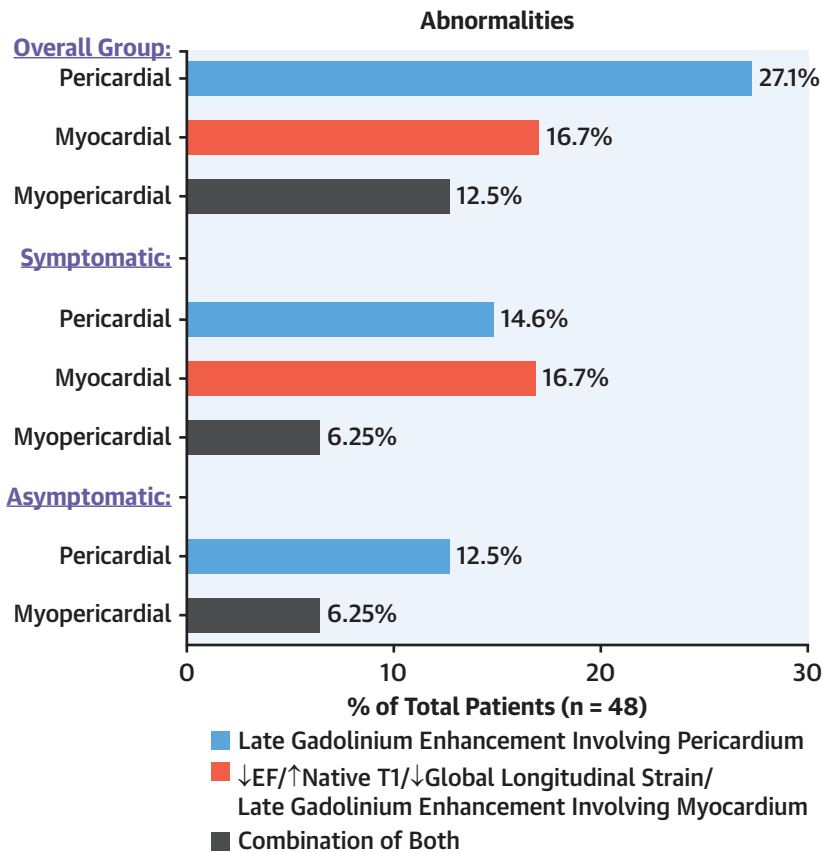
Brito, D. et al. J Am Coll Cardiol Img. 2021;14(3):541–55.

Data are presented as percentage of the total symptomatic/asymptomatic patients with coronavirus disease-2019 (COVID-19) who underwent both echocardiography and cardiac magnetic resonance, (n = 48). The definition of different cardiac involvements is as follows: 1) pericardial: presence of late enhancement with pericardial effusion; 2) myocardial: presence of any of the following: a) left ventricular ejection fraction (EF) <50%, b) global longitudinal strain <16%, (c) late enhancement involving myocardium, and c) native T_1 increase ≥990 ms; and 3) myopericardial: combination of both myocardial and pericardial involvement.

To understand the association between echocardiography strain abnormalities and CMR, we performed unsupervised hierarchical clustering. A model that was based on 16-segmental longitudinal strain grouped patients into 3 major clusters (**Figure 6**). A phenotypic group on the left of the dendrogram (group A: diffuse myopericardial involvement) clustered 9 patients with widespread reduction in regional longitudinal strains. The phenotypic distribution of CMR findings in group A was significantly different from the rest of the dendrogram (p = 0.03). The phenotypic group on the right of the dendrogram clustered 27 patients, 9 (33%) with pericardial enhancement (group B: mild myopericardial

involvement) with a reduction in their regional longitudinal strain but preserved overall LV GLS. The remaining patients in the center (group C: mild pericardial involvement) included 11 patients, with pericardial abnormalities seen in 4 (36%) cases. Supplemental Figure 2 shows the correlations between CMR-derived segmental T_1 and speckle tracking echocardiography-derived segmental longitudinal strain.

DISCUSSION

To the best of our knowledge, this is the first study to use comprehensive echocardiography with speckle

FIGURE 6   Comparison of CMR and Echocardiographic Findings
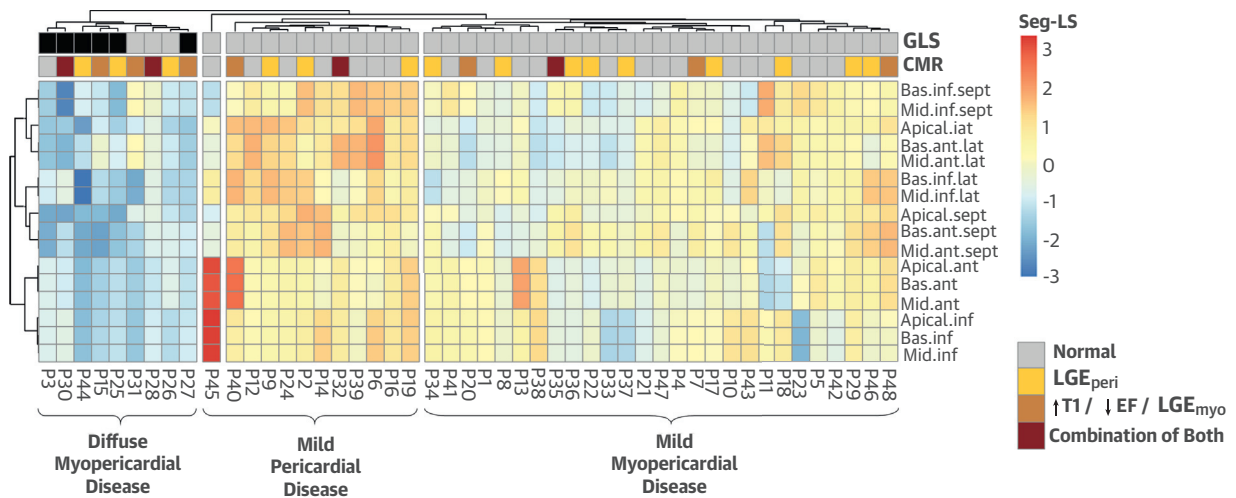
In the heatmap, the rows represent the different segmental strains, and the columns correspond to the patients. Euclidean measure for distance matrix and complete agglomeration method were applied to generate the cluster dendrograms on the **top** and the **left** of the heatmap. A *red-blue* color representation is used in presenting the relative intensity decrease in segmental strains across patients. The **top row** identifies the presence of abnormal global longitudinal strain (GLS) (<16, **black boxes**) from echocardiography. The **second row** identifies the category of cardiac magnetic resonance (CMR) abnormalities as shown in legend. ant = anterior; bas = basal; EF = ejection fraction; inf = inferior; LGE$_{myo}$ = late gadolinium enhancement involving myocardium; LGE$_{peri}$ = late gadolinium enhancement involving pericardium; seg-LS = segmental longitudinal strain; sept = septal; T$_1$ = native T$_1$.

tracking strain and CMR to explore the spectrum of cardiac involvement in college student athletes who recovered from uncomplicated COVID-19. Abnormal findings on cardiac imaging were seen in more than one-half of the patients, with 39.5% having pericardial late enhancement with pockets of pericardial effusion and patchy or a diffuse pattern of myocardial segmental strain abnormalities. Although the immediate and long-term clinical relevance of these findings remains unclear, our study underscores that mild or asymptomatic COVID-19 is not a benign illness, considering that more than one-half of the younger individuals showed subclinical myocardial and pericardial disease.

Recent CMR studies performed in adults convalescing from COVID-19 indicated a high prevalence of myocardial inflammation ([1,4]). In a recent study of 26 competitive athletes with COVID-19 that included 12 with mild symptoms and 14 asymptomatic athletes, CMR findings consistent with myocarditis on the basis of the presence of myocardial edema by elevated T$_2$ signal and myocardial injury shown by the presence of nonischemic delayed enhancements were reported in 4 (15%) athletes ([5]). In contrast, we observed a high prevalence of late pericardial enhancement. The normal pericardium is avascular,

and hence gadolinium uptake indicates signs of increased vascularity with pericardial inflammation. However, in our cohort, none of the patients had classic signs of acute inflammation (edema on CMR T$_2$ imaging or elevation of inflammatory biomarkers). Patients frequently showed residual pockets of pericardial effusion, a finding suggesting that this may represent a subacute or convalescing phase of pericarditis. It remains unclear whether the pericardial involvement seen in our study represents a primary viral involvement or identifies a more generalized COVID-19-related multisystemic inflammatory syndrome ([21]). During CMR imaging, we did not note additional involvement of serous surfaces such as the lung pleura in our cases. Interestingly, endothelial injury associated with intracellular SARS-CoV-2 has been described to cause new vessel growth, a unique mechanism referred to as intussusceptive angiogenesis ([22]). A potential susceptibility of pericardial mesothelial cells to SARS-CoV2 virus secondary to increased angiotensin-converting enzyme receptor activity coupled with inflammation and angiogenesis could explain the high prevalence of pericardial late enhancements and requires investigation ([23]).

COVID-19 can disrupt the cardiac contractile machinery and can cause unique patterns of LV

segmental dysfunction (24-27). Although the significance of these abnormalities is currently unclear, it is important for us to understand whether multimodality imaging can be used to identify clusters or subgroups of different pathophysiological phenotypes of COVID-19-induced cardiac involvement. Recent studies have used speckle tracking echocardiography–derived GLS with CMR for diagnosing the extent of myocardial dysfunction in viral myocarditis (28-30). Using similar multimodality imaging along with hierarchical clustering, an approach used previously to risk stratify COVID-19 patients (18), we identified 3 distinct phenotypic clusters in student athletes (**Figure 6**). However, the presence of a mere reduction in myocardial strain or an increase in native T_1 does not imply myocarditis because similar findings may result from inflammatory or takotsubo cardiomyopathy-like stress-induced myocardial dysfunction (31). More work is needed to establish the prognostic relevance of these phenotypic patterns.

Although direct myocardial or pericardial biopsy samples could establish these hypotheses, such investigative steps may be unreasonable for less symptomatic or asymptomatic individuals, considering that most patients with isolated CMR pericardial late enhancement would likely experience a benign course (32). A distinct 15% to 30% of patients could be at a risk of recurrent pericarditis or constrictive pericarditis (33). The presence of myocardial inflammation could have more severe consequences because chronic smoldering myocarditis could lead to the development of heart failure (34). In addition, the evidence of isolated nonischemic myocardial LGE on CMR can be a substrate for malignant arrhythmia and severe complications, such as sudden cardiac death (35). Therefore, until we have more information about the true nature of COVID-19-related illness, careful surveillance with cardiac imaging will be of paramount importance for identifying successful resolution or disease progression.

STUDY LIMITATIONS. First, although several studies have described delayed myocardial enhancement within the LV myocardium in ostensibly healthy athletes, the conservative estimates suggest that significant cardiac abnormalities are encountered in a frequency of 1:200 (0.5%) (36). The frequency and distribution of abnormalities in this confined group of young symptomatic and asymptomatic COVID-19 athletic students are therefore much higher than incidental findings reported in athletes from this age group. Second, because CMR was not clinically indicated in all asymptomatic athletes with COVID-19,

this could bias our observations on the true prevalence of subclinical findings in asymptomatic COVID-19. Third, although no subepicardial involvement was identified in LGE, the visceral pericardium is in extreme proximity, and a direct extension (less than a few pixels involvement) into the epicardium cannot be resolved. Fourth, although we used a multiple-step process to differentiate fat carefully from pericardial enhancements by using T_1 maps and B-SSFP cine images with confirmation offered by a second reader, a step using fat-saturated LGE could improve further confirmation of pericardial enhancement. Fifth, for COVID-19-related myopericardial involvement, we are unable to compare the direct prevalence estimate with other forms of viral infection. For example, PCR-confirmed H1N1 influenza can cause a high frequency of myocardial involvement in nearly one-third of patients (37). However, the prevalence and pathobiology of tissue inflammation are likely different in COVID-19 and influenza (22). Sixth, distinguishing an athlete's heart from myocardial disease is a conundrum pertinent to the present study. Although athletes can present with low-normal values for EF and preserved GLS (11), elevation of native T_1 or pericardial enhancements is not a routine feature of physiological adaptation. A recent study of 30 athletes reported marginally reduced native T_1 values in comparison with age-matched healthy control subjects (38). Similarly, although minimal pericardial effusions can be seen in athletes, these are not accompanied by features of late pericardial enhancement (39). Further testing with calculation of extracellular volume could be helpful. The lack of uniformly in collected hematocrit in all patients precluded us from estimating the extracellular volume from CMR T_1 mapping. The lack of CMR studies from a control athletic group makes it difficult to draw conclusions on the magnitude of CMR findings in athletic students with COVID-19. Finally, detailed clinical follow-up with imaging was unavailable for these patients at the time of the analysis. We used a plan for individualized assessments and the protocol for returning to play as outlined in the Supplemental Results section.

CONCLUSIONS

In a young, otherwise healthy cohort of college athletes recovering from COVID-19, myocardial and pericardial abnormalities were frequently identified using echocardiography and CMR. The presence of abnormal GLS and regional longitudinal strain identified the varying phenotypic patterns of myocardial involvement with a varying degree of regional

myocardial dysfunction. These data will help in developing future cardiac screening strategies and will guide serial testing in symptomatic and asymptomatic patients with COVID-19.

FUNDING SUPPORT AND AUTHOR DISCLOSURES

ADDRESS FOR CORRESPONDENCE: Dr. Partho P. Sengupta, West Virginia University Heart & Vascular Institute, 1 Medical Center Drive, Morgantown, West Virginia 26506, USA. E-mail: partho.sengupta@wvumedicine.org. Twitter: @ppsengupta1.

PERSPECTIVES

COMPETENCY IN MEDICAL KNOWLEDGE: Previously healthy college athletes recovering from COVID-19 have a high prevalence of CMR imaging findings that suggest resolving pericardial inflammation. CMR T_1 mapping and speckle tracking echocardiography also revealed subtle changes in myocardial structure and function.

TRANSLATIONAL OUTLOOK: Although specific clinical features of ongoing myocardial inflammation were not frequently identified, future studies are needed to address the underlying pathophysiological process and long-term evolution of the myo-pericardial abnormalities seen in uncomplicated COVID-19.

REFERENCES

1. Huang L, Zhao P, Tang D, et al. Cardiac involvement in patients recovered from COVID-2019 identified using magnetic resonance imaging. J Am Coll Cardiol Img 2020;13:2330–9.

2. Wang Y, Wang Y, Chen Y, Qin Q. Unique epidemiological and clinical features of the emerging 2019 novel coronavirus pneumonia (COVID-19) implicate special control measures. J Med Virol 2020;92:568–76.

3. Zhou F, Yu T, Du R, et al. Clinical course and risk factors for mortality of adult inpatients with COVID-19 in Wuhan, China: a retrospective cohort study. Lancet 2020;395:1054–62.

4. Puntmann VO, Carerj ML, Wieters I, et al. Outcomes of cardiovascular magnetic resonance imaging in patients recently recovered from coronavirus disease 2019 (COVID-19). JAMA Cardiol 2020;5:1265–73.

5. Rajpal S, Tong MS, Borchers J, et al. Cardiovascular magnetic resonance findings in competitive athletes recovering from COVID-19 infection. JAMA Cardiol 2021;6:116–8.

6. Lisboa Bastos M, Tavaziva G, Abidi SK, et al. Diagnostic accuracy of serological tests for COVID-19: systematic review and meta-analysis. BMJ 2020;370:m2516.

7. Centers for Disease Control and Prevention. Coronavirus disease 2019 (COVID-19): symptoms of coronavirus. 2020. Available at: https://www.cdc.gov/coronavirus/2019-ncov/symptoms-testing/symptoms.html. Accessed November 4, 2020.

8. World Medical Association. World Medical Association Declaration of Helsinki: ethical principles for medical research involving human subjects. JAMA 2013;310:2191–4.

9. Lang RM, Badano LP, Mor-Avi V, et al. Recommendations for cardiac chamber quantification by echocardiography in adults: an update from the American Society of Echocardiography and the European Association of Cardiovascular Imaging. J Am Soc Echocardiogr 2015;28:1–39.e14.

10. Rudski LG, Lai WW, Afilalo J, et al. Guidelines for the echocardiographic assessment of the right heart in adults: a report from the American Society of Echocardiography endorsed by the European Association of Echocardiography, a registered branch of the European Society of Cardiology, and the Canadian Society of Echocardiography. J Am Soc Echocardiogr 2010;23:685–713. quiz 786–8.

11. Baggish AL, Battle RW, Beaver TA, et al. Recommendations on the use of multimodality cardiovascular imaging in young adult competitive athletes: a report from the American Society of Echocardiography in Collaboration with the Society of Cardiovascular Computed Tomography and the Society for Cardiovascular Magnetic Resonance. J Am Soc Echocardiogr 2020;33:523–49.

12. Phelan D, Kim J, Elliott M, et al. Screening potential cardiac involvement in young athletes recovering from COVID-19: an international expert consensus statement. J Am Coll Cardiol Img 2020;13:2635–52.

13. Addis DR, Townsley MM. Imaging considerations for the athletically conditioned heart: an echocardiography-focused overview of the 2020 American Society of Echocardiography recommendations on the use of multimodality cardiovascular imaging in young adult competitive athletes. J Cardiothorac Vasc Anesth 2020;34:2867–70.

14. Wiesmueller M, Wuest W, Heiss R, Treutlein C, Uder M, May MS. Cardiac T2 mapping: robustness and homogeneity of standardized in-line analysis. J Cardiovasc Magn Reson 2020;22:39.

15. Piechnik SK, Ferreira VM, Dall'Armellina E, et al. Shortened modified look-locker inversion recovery (ShMOLLI) for clinical myocardial T1-mapping at 1.5 and 3 T within a 9 heartbeat breathhold. J Cardiovasc Magn Reson 2010;12:69.

16. Messroghli DR, Moon JC, Ferreira VM, et al. Clinical recommendations for cardiovascular magnetic resonance mapping of T1, T2, T2* and extracellular volume: a consensus statement by the Society for Cardiovascular Magnetic Resonance (SCMR) endorsed by the European Association for Cardiovascular Imaging (EACVI). J Cardiovasc Magn Reson 2017;19:75.

17. von Knobelsdorff-Brenkenhoff F, Schuler J, Doganguzel S, et al. Detection and monitoring of acute myocarditis applying quantitative cardiovascular magnetic resonance. Circ Cardiovasc Imaging 2017;10:e005242.

18. Mei Y, Weinberg SE, Zhao L, et al. Risk stratification of hospitalized COVID-19 patients through

comparative studies of laboratory results with influenza. EClinicalMedicine 2020;26:100475.

19. Ferreira VM, Schulz-Menger J, Holmvang G, et al. Cardiovascular magnetic resonance in non-ischemic myocardial inflammation: expert recommendations. J Am Coll Cardiol 2018;72:3158–76.

20. National Institutes of Health. COVID-19 treatment guidelines panel. coronavirus disease 2019 (COVID-19) treatment guidelines. Available at: https://www.covid19treatmentguidelines.nih.gov/. Accessed August 25, 2020.

21. Feldstein LR, Rose EB, Horwitz SM, et al. Multisystem inflammatory syndrome in U.S. children and adolescents. N Engl J Med 2020;383:334–46.

22. Ackermann M, Verleden SE, Kuehnel M, et al. Pulmonary vascular endothelialitis, thrombosis, and angiogenesis in Covid-19. N Engl J Med 2020;383:120–8.

23. Sousa IRF, Pereira ICC, Morais LJ, Teodoro L, Rodrigues MLP, Gomes R. Pericardial parietal mesothelial cells: source of the angiotensin-converting-enzyme of the bovine pericardial fluid. Arq Bras Cardiol 2017;109:425–31.

24. Chao CJ, DeValeria PA, Sen A, et al. Reversible cardiac dysfunction in severe COVID-19 infection, mechanisms and case report. Echocardiography 2020;37:1465–9.

25. Goerlich E, Gilotra NA, Minhas AS, Bavaro N, Hays AG, Cingolani OH. Prominent longitudinal strain reduction of basal left ventricular segments in patients with COVID-19. J Card Fail 2021;27:100–4.

26. Lairez O, Blanchard V, Houard V, et al. Cardiac imaging phenotype in patients with coronavirus disease 2019 (COVID-19): results of the cocarde study. Int J Cardiovasc Imaging 2020 Sep 9 [E-pub ahead of print].

27. Perez-Bermejo JA, Kang S, Rockwood SJ, et al. SARS-CoV-2 infection of human iPSC-derived cardiac cells predicts novel cytopathic features in hearts of COVID-19 patients. bioRxiv [Pre-print] 2020 Sep 12. 2020.08.25.265561.

28. Kasner M, Aleksandrov A, Escher F, et al. Multimodality imaging approach in the diagnosis of chronic myocarditis with preserved left ventricular ejection fraction (MCpEF): the role of 2D speckle-tracking echocardiography. Int J Cardiol 2017;243:374–8.

29. Leitman M, Vered Z, Tyomkin V, et al. Speckle tracking imaging in inflammatory heart diseases. Int J Cardiovasc Imaging 2018;34:787–92.

30. Uzieblo-Zyczkowska B, Mielniczuk M, Ryczek R, Krzesinski P. Myocarditis successfully diagnosed and controlled with speckle tracking echocardiography. Cardiovasc Ultrasound 2020;18:19.

31. Meyer P, Degrauwe S, Van Delden C, Ghadri JR, Templin C. Typical takotsubo syndrome triggered by SARS-CoV-2 infection. Eur Heart J 2020;41:1860.

32. Imazio M, Pivetta E, Palacio Restrepo S, et al. Usefulness of cardiac magnetic resonance for recurrent pericarditis. Am J Cardiol 2020;125:146–51.

33. Cremer PC, Kumar A, Kontzias A, et al. Complicated pericarditis: understanding risk factors and pathophysiology to inform imaging and treatment. J Am Coll Cardiol 2016;68:2311–28.

34. Escher F, Westermann D, Gaub R, et al. Development of diastolic heart failure in a 6-year follow-up study in patients after acute myocarditis. Heart 2011;97:709–14.

35. Zorzi A, Perazzolo Marra M, Rigato I, et al. Nonischemic left ventricular scar as a substrate of life-threatening ventricular arrhythmias and sudden cardiac death in competitive athletes. Circ Arrhythm Electrophysiol 2016;9:e004229.

36. La Gerche A, Baggish AL, Knuuti J, et al. Cardiac imaging and stress testing asymptomatic athletes to identify those at risk of sudden cardiac death. J Am Coll Cardiol Img 2013;6:993–1007.

37. Mavrogeni S, Bratis C, Kitsiou A, et al. CMR assessment of myocarditis in patients with cardiac symptoms during H1N1 viral infection. J Am Coll Cardiol Img 2011;4:307–9.

38. McDiarmid AK, Swoboda PP, Erhayiem B, et al. Athletic cardiac adaptation in males is a consequence of elevated myocyte mass. Circ Cardiovasc Imaging 2016;9:e003579.

39. Domenech-Ximenos B, Sanz-de la Garza M, Prat-Gonzalez S, et al. Prevalence and pattern of cardiovascular magnetic resonance late gadolinium enhancement in highly trained endurance athletes. J Cardiovasc Magn Reson 2020;22:62.

KEY WORDS athletes, CMR, COVID-19, echocardiography, strain

APPENDIX For supplemental Methods and Results sections as well as supplemental table, figures, and videos, please see the online version of this paper.